ORIGINAL PAPER

RJME
Romanian Journal of Morphology & Embryology
http://www.rjme.ro/

Optical biopsy strategy for the assessment of atrophic gastritis, intestinal metaplasia, and dysplasia

SILVIA COSMINA DRAŞOVEAN[1)], ALINA MIOARA BOERIU[1)], PETER SELASE AKABAH[1)], SIMONA LILIANA MOCAN[2)], OFELIA DANIELA PASCARENCO[1)], ECATERINA DANIELA DOBRU[1)]

[1)]*Department of Gastroenterology, University of Medicine and Pharmacy of Tîrgu Mureş, Romania*
[2)]*Department of Pathology, Emergency County Hospital, Tîrgu Mureş, Romania*

Abstract

Background and aims: The pathogenesis of gastric cancer involves premalignant changes of the gastric mucosa. An accurate estimation of the topography and severity of these lesions represents an important step in detecting premalignant lesions, thereby classifying patients into low or high risk of developing gastric cancer. We prospectively analyzed the diagnostic performance of narrow-band imaging with magnification endoscopy (NBI-ME) for assessing premalignant gastric lesions during real-time examination. *Patients, Materials and Methods*: A total number of 59 patients were examined by NBI-ME and target biopsies of the antrum, corporeal, and *incisura angularis* levels. Modified endoscopic patterns were classified into three groups: type A [tubulo-villous mucosal pattern with regular microvessels, or the light blue crest (LBC) sign], type B [disappearance of normal subepithelial capillary network (SECN) pattern], and type C [irregular mucosal pattern (IMP) and/or irregular vascular pattern (IVP)]. The endoscopic diagnosis was compared to histological findings (the gold standard). The NBI-ME results were assessed for accuracy, sensitivity, specificity, and negative and positive predictive values in detecting intestinal metaplasia, atrophic gastritis and dysplasia. *Results*: Analysis of endoscopic patterns showed a good correlation with premalignant lesions ($p<0.05$). Type A pattern showed 80.2% accuracy, 80.43% sensitivity and 80% specificity [area under receiver operating characteristic (AUROC) of 0.8] in detecting intestinal metaplasia. Diagnostic performance for assessment of atrophic gastritis was not ideal (69.5% accuracy, 83.72% sensitivity, 56.04% specificity, AUROC 0.69). Pattern C represents a reliable endoscopic marker for the diagnosis of dysplasia (91.1% accuracy, 83.3% sensitivity, 91.81% specificity, AUROC 0.87). The extension of precancerous lesions was estimated during endoscopic examination. *Conclusions*: NBI-ME represents a valuable tool in the assessment of premalignant gastric lesions, thereby categorizing patients into low and high risks of developing gastric cancer. The applicability of the method in routine practice is promising, as it helps shape the follow up protocol of patients with premalignant lesions of the stomach. It is worth mentioning that, this method requires standardization, additional training, and expertise.

Keywords: atrophic gastritis, intestinal metaplasia, dysplasia, narrow-band imaging, optical biopsy.

Introduction

Gastric cancer remains a major cause of morbidity and mortality worldwide. The development of gastric cancer is a multistep process, consisting in inflammatory changes of gastric mucosa, which may progress to atrophic and metaplastic transformation, followed by dysplasia and gastric adenocarcinoma [1].

The risk of the patient for the development of gastric cancer is mainly related to the intragastric extent and severity of premalignant gastric lesions [2, 3]. Current practice requires an important number of biopsies and costly histopathology analysis for proper assessment of these parameters by white-light endoscopy [4]. Even so, an accurate estimation of the lesions may be difficult due to their multifocal and patchy distribution.

New modalities to facilitate the detection and surveillance of premalignant gastric lesions have been developed during recent years. Narrow-band imaging (NBI) represents an advanced endoscopic technique that enhances visualization of pit pattern and vascular details of the mucosal by using narrow wavelength bands [5, 6]. Combination with magnification endoscopy (NBI-ME) provides the opportunity to improve the detection and characterization of lesions and a real-time estimation of underlying histology.

A number of important studies have been performed that were focused on the usefulness of the method for the diagnosis of gastric intestinal metaplasia, atrophic gastritis, dysplasia, as well as for gastric neoplasia [7, 8]. Various vascular and mucosal patterns have been described to be associated with premalignant gastric lesions. However, standardization and experience are required to establish an accurate diagnosis [9–11].

The primary aim of this study was to evaluate the clinical usefulness of NBI-magnifying endoscopy in the detection and characterization of premalignant gastric lesions. A prospective evaluation of the performance of real-time optical biopsy was carried out, by using specific endoscopic criteria. The secondary aim was to test the ability of the method to estimate the intragastric extension of precancerous lesions.

Patients, Materials and Methods

Study population

We performed endoscopic examination with NBI-ME in a convenience sample population of 59 patients with ages between 31 and 80 years old (mean age of 59.5± 10.26 years old) with dyspeptic symptoms. The patients were admitted in the Clinic of Gastroenterology,

Emergency County Hospital, Tîrgu Mureş, Romania, during a one-year period, from May 2016 to May 2017. The majority of the patients (62%) were from the urban area. Patients in the sample population provided a written, informed consent for all procedures. Exclusion criteria from the study population were coagulation disorders, anticoagulant therapy, severe pulmonary, cardiovascular, liver and renal comorbidities, psychiatric disorders, gastric surgery or malignancy. The study protocol was approved by the Ethics Committee at our Institution.

Endoscopy procedure

A high-definition magnification endoscope with an NBI system and dual-focus optical imaging (EvisExera III, GIF-HQ190, Olympus) was used in the study. Three endoscopists with experience in NBI technique performed all endoscopic procedures. During the procedures, patients were sedated with Propofol by a registered anesthesiologist.

Endoscopic and histopathological diagnosis

Endoscopic diagnosis was established by subsequent evaluation of pit pattern of the mucosal and vascular patterns at the antral, corporeal and *incisura angularis* levels. Modified endoscopic patterns were classified into three main distinct types according to specific mucosal and vascular features:

▪ Type A: areas presenting either a tubulo-villous mucosal pattern with regular microvessels, or the light blue crest (LBC) sign. LBC appears as blue-whitish, slightly raised areas under NBI-ME.

▪ Type B: areas with the disappearance of normal subepithelial capillary network (SECN).

▪ Type C: areas showing an irregular mucosal pattern (IMP) and/or an irregular vascular pattern (IVP), represented by mucosal architectural distortion and/or changes in the size, shape, and distribution of microvessels NBI-ME target examination of mucosal and vascular patterns at the antral level (A), corporeal level (C) and *incisura angularis* (IA) was successively performed. Targeted biopsies were obtained from suspicious areas with modified patterns. In the absence of any detectable modified pattern, random biopsies were taken from normal mucosa at A, C, and IA level. Biopsies from distinct anatomical regions were separately labeled (A, C, and IA) and send to the Department of Histopathology. Real-time endoscopic diagnosis of presumed premalignant lesion was made during the examinations. Endoscopic reports contained a full description of pit pattern of mucosa and vascular patterns and their anatomical locations. Endoscopic diagnosis was compared with histopathology results acting as the gold standard.

Histological analysis was performed by an experienced gastrointestinal pathologist. Gastric bioptic specimens were fixed in formalin, embedded in paraffin, sectioned, and stained with Hematoxylin and Eosin (HE).

For the assessment of the inflammatory reaction of the gastric mucosa and the presence of *Helicobacter pylori* bacteria, from the biological material included in paraffin there were performed serial sections in the microtome, subsequently placed on poly-L-lysine covered slides and subjected to the immunohistochemical (IHC) marking protocol. In our study, we used the following markers: anti-CD3 (monoclonal mouse anti-human D3, clone F7.2.38, 1:50 dilution, Dako) for the assessment of T-lymphocytes presence, anti-CD20 (monoclonal mouse anti-human CD20cy, clone L26, 1:50 dilution, Dako) for highlighting B-lymphocytes, anti-CD79α (monoclonal mouse anti-human CD79α, clone JCB117, 1:50 dilution, Dako) for assessing plasmocytes and the anti-*H. pylori* antibody (rabbit *H. pylori*, clone ab140128, 1:100 dilution, Abcam).

Atrophic gastritis and intestinal metaplasia were assessed and graded according to a visual analog scale in the updated Sydney System [12]. Dysplasia was assessed according to the current *World Health Organization* (WHO) classification [13].

Statistical analysis

Statistical analysis was performed using the MedCalc software ver. 12.5.0.0. Qualitative data was presented as counts and percentages. The association between qualitative variables was assessed using the χ^2 (*chi*-square) test or the Fisher's exact test. A per-lesion analysis was performed to determine the diagnosis accuracy, sensitivity (Se), specificity (Sp), and predictive value (PV) of specific NBI endoscopic criteria for intestinal metaplasia, atrophic gastritis, and dysplasia. Likelihood ratios for a positive result (+LR) and for a negative result (–LR) were estimated. The diagnostic performance of endoscopic method was evaluated by area under receiver operating characteristic (AUROC) curves. For all the statistical tests, the significance level α was set at 0.05 and the two-tailed *p*-value was computed.

Results

A total of 59 patients were included in our study (26 men, 33 women), with mean age 59.50±10.26 years old (range 31–80 years old). One hundred and seventy-seven distinct areas were examined by applying magnifying high-definition NBI and targeted biopsies.

The topography of detected endoscopic patterns is presented in Table 1.

Table 1 – ***Topography of modified endoscopic patterns (per-patient assessment)***

Location		Tubulo-villous pattern/ LBC sign	Disappearance of SECN pattern	IMP	IVP
		N (%) patients	*N (%) patients*	*N (%) patients*	*N (%) patients*
A		32 (54.2)	43 (72.9)	7 (11.9)	4 (6.8)
IA		25 (42.4)	30 (50.8)	2 (3.4)	2 (3.4)
C		12 (20.3)	12 (20.3)	8 (13.6)	7 (11.9)
Extensive lesions	*Two areas*	16 (27.1)	24 (40.7)	–	–
	Three areas	7 (11.9)	7 (11.9)	–	–

A: Gastric antrum; IA: *Incisura angularis*; C: Gastric corpus; LBC: Light blue crest; SECN: Subepithelial capillary network; IMP: Irregular mucosal pattern; IVP: Irregular vascular pattern; *N*: No. of cases.

The majority of modified areas were identified at the antral level (type A pattern in 32 patients, type B in 43, IMP in seven, and IVP in four patients). Type A and type B patterns were detected at the corporeal level in 12 patients each, while IMP and IVP in gastric corpus were examined in eight and seven patients, respectively. Regarding the real-time estimation of the intragastric extension of lesions by NBI, we investigated patients in which modified areas were detected in at least two gastric locations (antrum, corpus and/or *incisura angularis*). Type A pattern was detected in two distinct gastric locations in 16 patients and type B pattern in 24 patients. Type A and type B patterns localized in three distinct gastric regions were identified in seven patients.

We analyzed the correspondence between endoscopic patterns and histology results. We presumed that type A pattern corresponds with intestinal metaplasia, while type C pattern is an indicator of dysplasia. An analysis of those areas presenting the type B pattern, with or without concurrent type A pattern, as indicators of atrophic gastritis, was also performed. Per-lesion analysis revealed that from 91 lesions endoscopically suspected for intestinal metaplasia (IM) (type A pattern), in 74 the diagnosis of IM was confirmed. Only in 56 of 85 areas presenting type B pattern, histology confirmed atrophic gastritis. From 112 areas presenting type A pattern and/or the type B pattern, atrophic gastritis was diagnosed by histology in 72 areas. From 19 areas showing type C pattern, dysplasia was confirmed in six areas (Table 2).

Table 2 – ***Correspondence between endoscopic findings and histology results (per-lesion assessment)***

Endoscopy	Histology		
	Intestinal metaplasia	***Atrophic gastritis***	***Dysplasia***
N (%) areas	*N (%) areas*	*N (%) areas*	*N (%) areas*
Type A pattern: 91 (51.4)	74 (41.8)	–	–
Type B pattern: 85 (48)	–	56 (31.63)	–
Type A/type B pattern: 112 (63.3)	–	72 (40.67)	–
Type C pattern: 19 (10.7)	–	–	6 (3.38)

N: No. of cases.

Endoscopic features (type A, type B, and type C patterns) were significantly associated ($p<0.0001$) with the diagnosis of premalignant gastric lesions (intestinal metaplasia, atrophic gastritis, and dysplasia).

The topography of lesions

We performed a per-patient analysis of topography of premalignant lesions. The anatomic distribution of IM, atrophic gastritis (AG), and dysplasia diagnosed by targeted NBI examination and biopsies was assessed. The results are depicted in Table 3.

We defined as extensive premalignant gastric lesions those areas where IM and/or AG were detected in at least two gastric locations. NBI-ME allowed the identification of 16 (27%) patients with extensive IM; 13 (22%) patients had extensive AG. Dysplasia was diagnosed in one patient at the antral level and in five (8.5%) patients at the corporeal level.

Table 3 – ***Topography of premalignant gastric lesions detected by NBI-ME and targeted biopsies (per-patient assessment)***

Location		Atrophic gastritis	Intestinal metaplasia	Dysplasia
		N (%) patients	***N (%) patients***	***N (%) patients***
A		37 (62.7)	41 (69.5)	1 (1.7)
IA		28 (47.5)	29 (49.2)	–
C		21 (35.6)	22 (37.3)	5 (8.5)
Extensive lesions	Two areas	13 (22)	16 (27.1)	–
	Three areas	13 (22)	14 (23.7)	–

NBI-ME: Narrow-band imaging with magnification endoscopy; A: Gastric antrum; IA: *Incisura angularis*; C: Gastric corpus; *N*: No. of cases.

The assessment of intestinal metaplasia

We analyzed the diagnostic performance of NBI-ME in the real-time estimation of IM. The results are depicted in Table 4.

Table 4 – ***Diagnostic performance of NBI-ME in detecting intestinal metaplasia***

Diagnostic performance	Endoscopic patterns		
	LBC sign	***Tubulo-villous pattern***	***Type A pattern***
Accuracy [%]	69.4	72.3	80.2
Se [%] (95% CI)	47.83 (37.3–58.5)	60.87 (50.1–70.9)	80.43 (70.9–88)
Sp [%] (95% CI)	92.94 (85.3–97.4)	84.71 (75.3–91.6)	80 (69.9–87.9)
PPV [%] (95% CI)	88 (75.5–95.5)	81.2 (69.9–89.6)	81.3 (71.7–88.8)
NPV [%] (95% CI)	62.2 (53.2–70.7)	66.7 (56.9–75.4)	79.1 (69–87.1)
+LR (95% CI)	6.78 (5.4–8.5)	3.98 (3.3–4.8)	4.02 (3.5–4.7)
–LR (95% CI)	0.56 (0.3–1.2)	0.46 (0.3–0.8)	0.24 (0.1–0.4)
AUROC (95% CI)	0.704 (0.631–0.77)	0.728 (0.656–0.792)	0.802 (0.736–0.858)
Standard error	0.02	0.03	0.03
P-value	<0.0001	<0.0001	<0.0001

NBI-ME: Narrow-band imaging with magnification endoscopy; Se: Sensitivity; CI: Confidence interval; Sp: Specificity; PPV: Positive predictive value; NPV: Negative predictive value; +LR: Positive likelihood ratio; –LR: Negative likelihood ratio; AUROC: Area under receiver operating characteristic; LBC: Light blue crest.

LBC sign and tubulo-villous pattern were considered predictive endoscopic features for IM (Figures 1 and 2). From 50 areas exhibiting LBC sign at NBI-ME, IM was confirmed in 44 (88%) areas. The accuracy, Se, Sp, PPV and NPV of LBC sign for the detection of IM were 69.4%, 47.83%, 92.94%, 88%, and 62.2%, respectively. A total of 69 areas with tubulo-villous patterns were analyzed. Histology confirmed IM in 56 (81%) of these areas (Figure 3). Tubulo-villous pattern with regular micro-vessels showed a 72.3% accuracy, 60.87% Se and 84.71% Sp, 81.2% PPV and 66.7% NPV in diagnosing IM.

The overall accuracy of both of these two endoscopic criteria (type A pattern) in detecting IM was 80.2%, with 80.43% Se, 80% Sp, 81.3% PPV, 79.1% NPV, and positive likelihood ratio LR+ 4.02 respectively. Area under curve (AUC) in receiver operating characteristic (ROC) curve was 0.8 when any one of these two endoscopic criteria was used.

The assessment of atrophic gastritis

Table 5 presents the diagnostic performance of NBI-ME in evaluating AG. Areas containing a loss of normal SECN pattern (type B pattern), LBC sign and/or tubulo-villous pattern (type A pattern) were analyzed for the detection of AG. A total of 85 areas showing the disappearance of normal SECN pattern (type B pattern) were biopsied. The histological confirmation of AG was achieved in 56 (65.8%) areas. The accuracy, Se, Sp, PPV, NPV, and +LR of type B pattern were 66.6%, 65.12%, 68.13%, 65.9%, 67.4%, and 2.04, respectively. AUROC was 0.66.

Table 5 – ***Diagnostic performance of NBI-ME in detecting atrophic gastritis***

Diagnostic performance	Endoscopic patterns	
	Type B pattern	*Type A/Type B pattern*
Accuracy [%]	66.6	–
Se [%] (95% CI)	65.12 (54.1–75.1)	83.72 (74.2–90.8)
Sp [%] (95% CI)	68.13 (57.5–77.5)	56.04 (45.2–66.4)
PPV [%] (95% CI)	65.9 (54.8–75.8)	64.3 (54.7–73.1)
NPV [%] (95% CI)	67.4 (56.8–76.8)	78.5 (66.4–87.8)
+LR (95% CI)	2.04 (1.7–2.5)	1.9 (1.6–2.3)
–LR (95% CI)	0.51 (0.3–0.8)	0.29 (0.2–0.5)
AUROC (95% CI)	0.666 (0.592–0.735)	0.699 (0.625–0.765)
Standard error	0.03	0.03
P-value	<0.0001	<0.0001

NBI-ME: Narrow-band imaging with magnification endoscopy; Se: Sensitivity; CI: Confidence interval; Sp: Specificity; PPV: Positive predictive value; NPV: Negative predictive value; +LR: Positive likelihood ratio; –LR: Negative likelihood ratio; AUROC: Area under receiver operating characteristic.

When we analyzed those areas presenting either the type A pattern (tubulo-villous mucosa/LBC sign) or the type B pattern (loss of normal SECN), as potential markers of AG, we obtained 69.5% diagnostic accuracy, 83.72% Se, 56.04% Sp, 64.3% PPV, 78.5% NPV, and +LR 1.9 of these combined endoscopic criteria in detecting gastric atrophy. AUROC was 0.69.

A distinct analysis for the assessment of corporeal AG was performed. We detected 31 areas showing type A and/or type B patterns at the corporeal level (Figure 4). Histology confirmed atrophy in 21 (67.7%) of these cases (Figure 5). The diagnostic accuracy of corporeal AG was 70.6%, with 33.33% Se, 91.23% Sp, 67.7% PPV, 71.2% NPV, +LR 3.8, when any one of three endoscopic criteria was assessed.

The assessment of dysplasia

The diagnostic performance of NBI-ME in evaluating dysplasia was investigated as depicted in Table 6.

Table 6 – ***Diagnostic performance of NBI-ME in detecting dysplasia***

Diagnostic performance	Endoscopic patterns		
	IMP	*IVP*	*Type C pattern*
Accuracy [%]	92.6	94.9	91.1
Se [%] (95% CI)	83.33 (35.9–99.6)	83.33 (35.9–99.6)	83.33 (35.9–99.6)
Sp [%] (95% CI)	92.98 (88.1–96.3)	95.32 (91–98)	91.81 (86.6–95.5)
PPV [%] (95% CI)	29.4 (10.3–56)	38.5 (13.9–68.4)	26.3 (8.8–52)
NPV [%] (95% CI)	99.4 (96.6–100)	99.4 (96.6–100)	99.4 (96.5–100)
+LR (95% CI)	11.88 (8.3–17)	17.81 (12.4–25.5)	10.18 (7.1–14.6)
–LR (95% CI)	0.18 (0.03–1.2)	0.17 (0.03–1.2)	0.18 (0.03–1.2)
AUROC (95% CI)	0.882 (0.825–0.925)	0.893 (0.838–0.935)	0.876 (0.818–0.92)
Standard error	0.08	0.08	0.08
P-value	<0.0001	<0.0001	<0.0001

NBI-ME: Narrow-band imaging with magnification endoscopy; Se: Sensitivity; CI: Confidence interval; Sp: Specificity; PPV: Positive predictive value; NPV: Negative predictive value; +LR: Positive likelihood ratio; –LR: Negative likelihood ratio; AUROC: Area under receiver operating characteristic; IMP: Irregular mucosal pattern; IVP: Irregular vascular pattern.

We detected 17 areas showing an IMP, and 13 areas with an IVP (Figure 6). The accuracy of IMP for the diagnosis of dysplasia was 92.6%, with 83.33% Se, 92.98% Sp, 29.4% PPV, and 99.4% NPV. IVP showed 94.9% accuracy, 83.33% Se, 95.32% Sp, 38.5% PPV, and 99.4% NPV in diagnosing dysplasia.

The appearance of either IMP or IVP (type C pattern) was detected in 19 areas. Histological confirmation of dysplasia was obtained in six (31.5%) of these areas (Figure 7). Type C pattern showed 91.1% diagnostic accuracy, 83.3% Se, 91.81% Sp, 26.3% PPV, 99.4% NPV, and +LR 10.18, respectively). AUROC was 0.87.

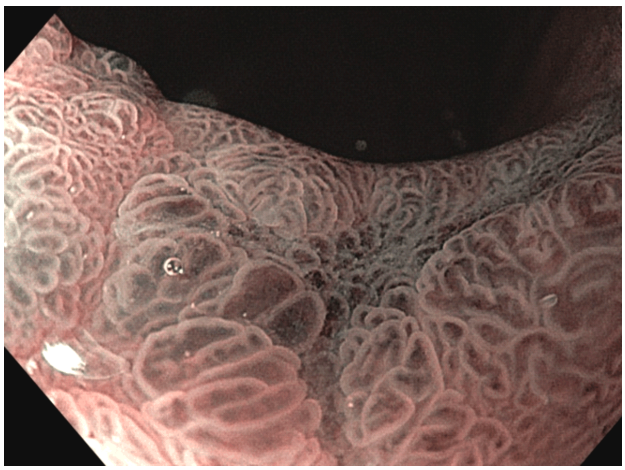

Figure 1 – ***Tubulo-villous pattern with blue-whitish, slightly raised areas (type A pattern; intestinal metaplasia).***

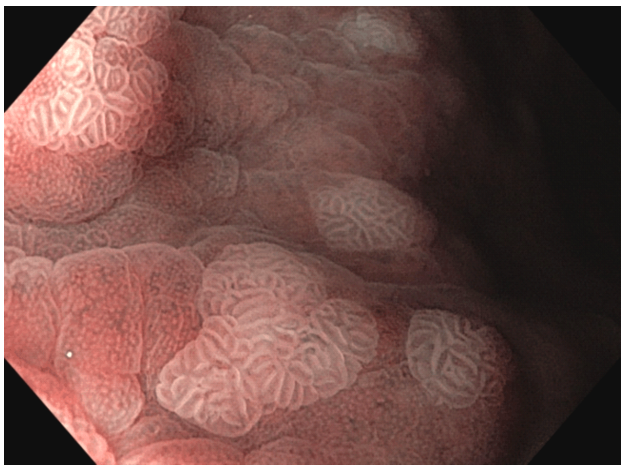

Figure 2 – ***Multiple blue-whitish, slightly raised areas (LBC sign; extensive intestinal metaplasia). LBC: Light blue crest.***

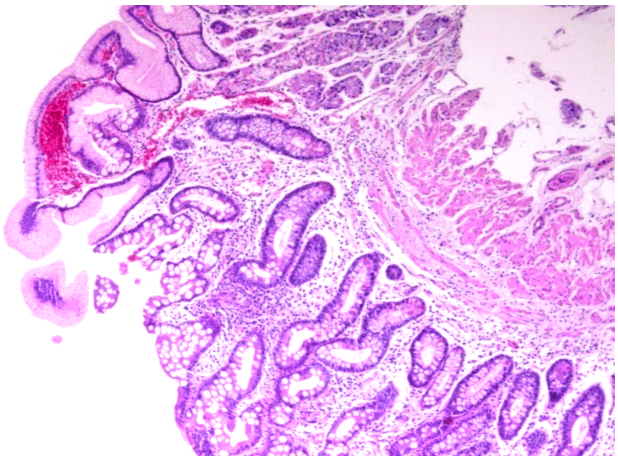

Figure 3 – ***Intestinal metaplasia with corporeal atrophic gastritis [Hematoxylin-Eosin (HE) staining, ×50].***

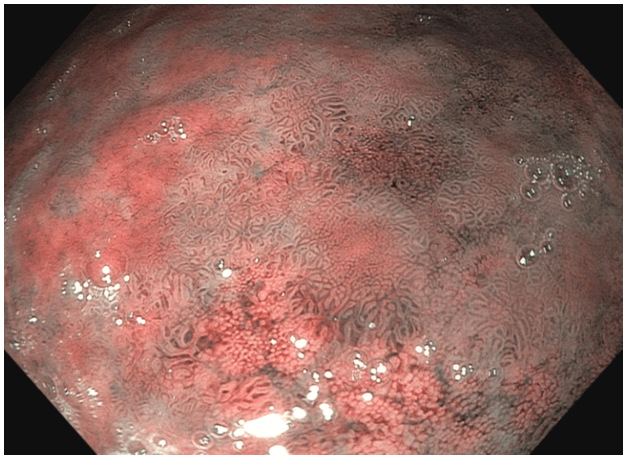

Figure 4 – ***Disappearance of normal SECN pattern and areas of tubulo-villous pattern (type A/type B pattern; extensive atrophic gastritis and intestinal metaplasia). SECN: Subepithelial capillary network.***

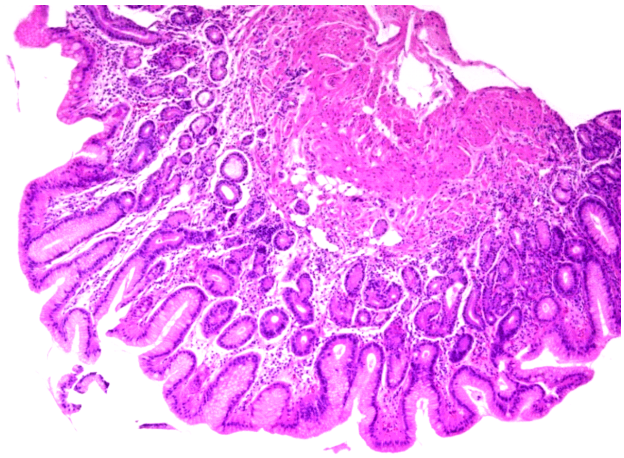

Figure 5 – ***Severe corporeal atrophic gastritis (HE staining, ×50).***

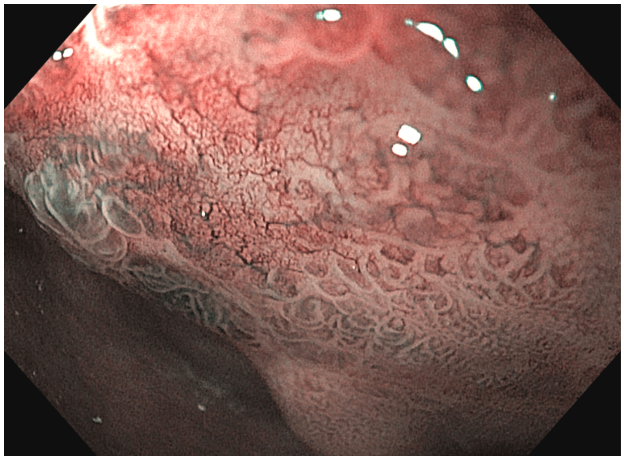

Figure 6 – ***Area presenting an irregular vascular pattern (type C pattern; dysplasia), nearby a regular tubulo-villous pattern (type A pattern; intestinal metaplasia).***

The IHC study highlighted a positive reaction for *H. pylori* in 37 (62.71%) patients (Figure 8) and negative in 22 (37.29%) patients (Figure 9). In the patients with positive *H. pylori* there were highlighted numerous cases of intestinal metaplasia. The inflammatory reaction of the gastric mucosa was more intense in the patients with positive *H. pylori*. The distribution of T- and B-lymphocytes was diffuse and completely heterogeneous in the gastric mucosa chorion, except for the areas with lymphoid follicles, where B-lymphocytes were numerous (Figures 10 and 11). In our study, we observed that plasmocytes were much more numerous, in comparison to T- and B-lymphocytes (Figure 12).

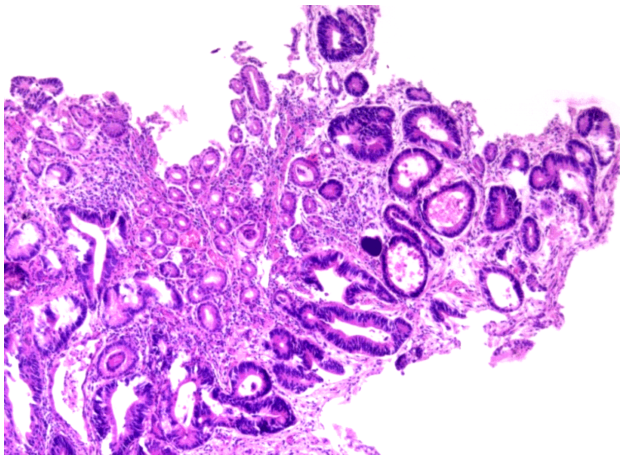

Figure 7 – ***Image of gastric mucosa with severe dysplasia (HE staining, ×50).***

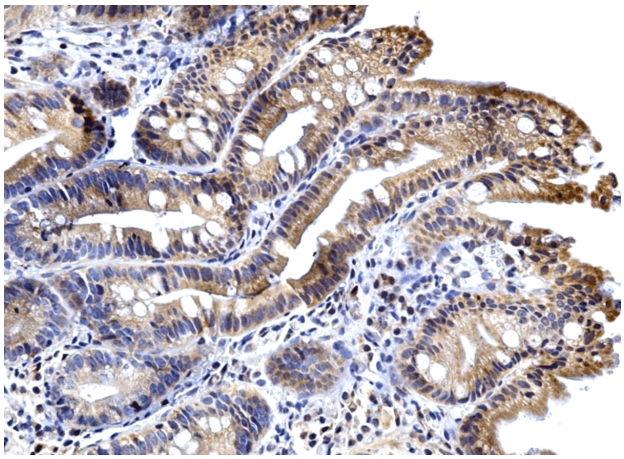

Figure 8 – ***Chronic gastritis with intestinal metaplasia and positive reaction to anti-Helicobacter pylori (HP) antibody (Immunomarking with anti-HP antibody, ×200).***

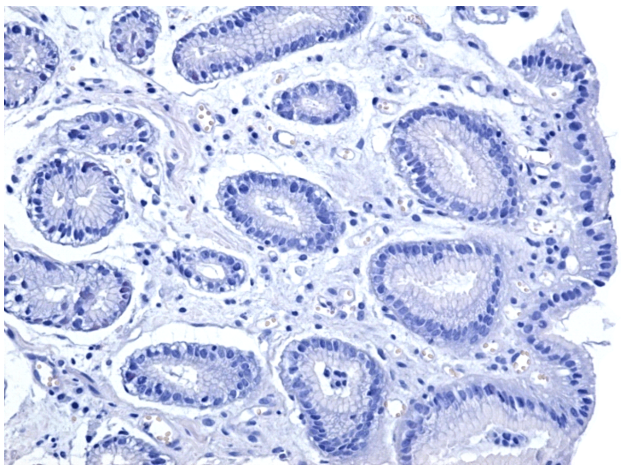

Figure 9 – ***Chronic atrophic gastritis with negative reaction to anti-HP antibody (Immunomarking with anti-HP antibody, ×200).***

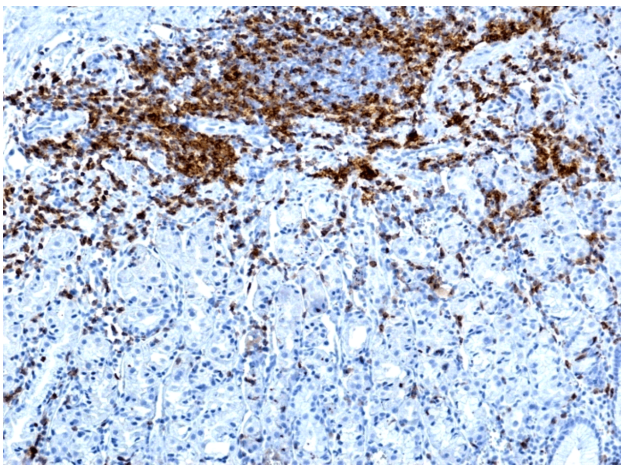

Figure 10 – ***Chronic gastritis positive to H. pylori, with numerous T-lymphocytes present in the deep chorion (Immunomarking with anti-CD3 antibody, ×100).***

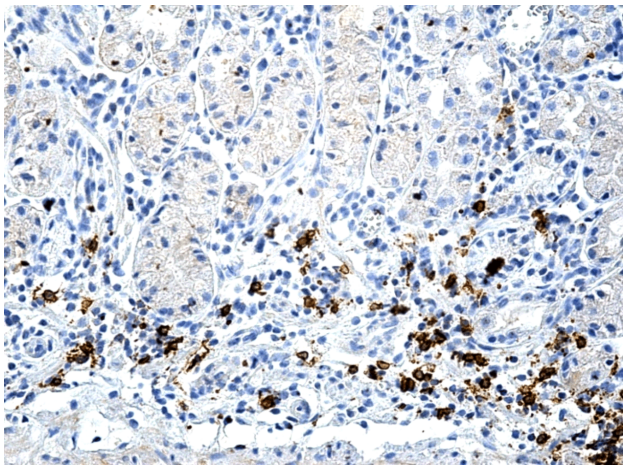

Figure 11 – ***Image of chronic gastritis with B-lymphocytes diffusely disseminated in chorion (Immunomarking with anti-CD20 antibody, ×200).***

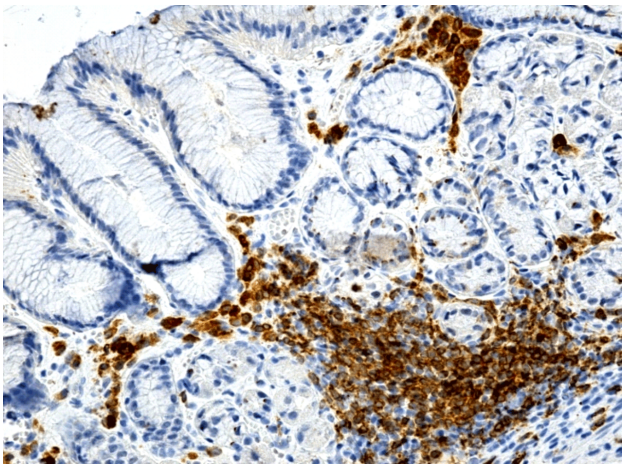

Figure 12 – ***Chronic gastritis with lamina propria infiltrated with plasma cells (Immunomarking with the anti-CD79α antibody, ×200).***

Discussions

The accurate estimation of the real extension of premalignant gastric lesions during conventional white-light endoscopy remains a challenge in clinical practice. A topographic mapping of gastric mucosa is recommended for the assessment of atrophic gastritis and intestinal metaplasia, consisting in multiple biopsy samples obtained from the antrum, corpus, and *incisura angularis*. Additional biopsies from any visible lesion are required. Even by applying the Sidney protocol, the premalignant lesions may be missed, due to their anatomic distribution. Also, most endoscopists do not routinely obtain the recommended number of biopsies. The detection of dysplasia is even more difficult, as the subtle changes at the level of the mucosa may be missed on white-light endoscopy.

The advent of new endoscopic modalities now allows an accurate detection and characterization of gastric lesions. Thus, a true optical biopsy is performed in real-time, by examining the gastric mucosa with NBI and magnification. The combination of NBI with magnification endoscopy enhances microvasculature details, allowing a more accurate differentiation between non-neoplastic and neoplastic gastric lesions than standard white-light endoscopy [14, 15].

Our research focused on the correspondence between endoscopy and histology, in order to prove the value of NBI optical diagnosis and its practical applicability. After reviewing the literature, we selected those endoscopic criteria most helpful for differentiating between normal gastric mucosa and premalignant lesions.

Many analyses of NBI endoscopic patterns have been performed in an attempt to create a simplified diagnostic algorithm, both accurate and reproducible in current practice [16, 17]. Pimentel-Nunes *et al.* developed and validated a simplified NBI classification for differentiation of premalignant lesions. Regular and circular mucosal patterns with regular vascular patterns correspond with normal mucosa [accuracy 83%; 95% confidence interval (CI) 75–90%]. Regular, ridge or tubulo-villous mucosal patterns with regular vessels are highly associated with IM (accuracy 84%; 95% CI 77–91%). Absent or irregular mucosal patterns and irregular vascular patterns represent reliable markers for dysplasia (accuracy 95%; 95% CI 90–99%) [16].

The LBC sign was first described by Uedo *et al.* as reliable endoscopic criteria for the detection of IM [17]. The authors reported excellent sensitivity (89%), specificity (93%) and diagnostic accuracy (91%) [18]. In a recent meta-analysis, four studies have been evaluated for the

diagnostic performance of NBI-ME on a per-lesion basis; the pooled sensitivity to differentiate IM was 0.69 (0.63 to 0.74) and the pooled specificity was 0.91 (0.87 to 0.94) [19].

In our analysis, we obtained a good specificity (92.94%) of the LBC sign for IM, but a low sensitivity (47.83%). In practice, both the LBC sign and the tubulo-villous pattern (classified as type A pattern in our study) are used as endoscopic markers for IM. The overall accuracy of type A pattern in diagnosing IM was 80.2%, with a likelihood ratio of 4.02, a good sensitivity and specificity (AUROC 0.8).

The presence of the LBC sign at the level of gastric mucosa of the greater curvature of the antrum and corpus has been described as a predictor of severity of AG [20]. Anagnostopoulos *et al.* identified the disappearance of the normal honeycomb-like SECN, the presence of irregular collecting venules, as well as areas of tubular structures in the gastric body mucosa in patients with autoimmune gastritis evaluated by high-resolution magnification endoscopy [20, 21]. Villous surface pattern and irregular narrowed coiled subepithelial capillaries detected on NBI-ME were associated with severe atrophic changes and IM in other reports [22]. Following this evidence, we examined our patients exhibiting similar patterns on NBI-ME (the loss of normal SECN pattern, the presence of extensive areas displaying either the LBC sign or the tubulo-villous pattern), as presumptive indicators of AG. We found that the diagnostic performance of the endoscopic features associated with AG is not ideal. Diagnostic accuracy was 69.5%, sensitivity was 83.72%, and AUROC was 0.69, when any one of these three criteria was present (Type A/type B pattern). When we analyzed these endoscopic features at the level of gastric body, the diagnostic accuracy for corporeal AG was 70.6%, with an increased specificity (91.23%), but low sensitivity (33.33%). The disappearance of normal SECN pattern (type B pattern) alone showed only 66.6% accuracy, 65.12% Se, and 68.13% Sp for gastric atrophy. In fact, the loss of the normal vascular pattern by replacement with an irregular microvascular pattern has also been described as an endoscopic pattern in dysplastic lesions.

Differences between endoscopic and histological diagnosis of atrophy may be explained by an inadequate biopsy tissue sampling. Superficial biopsy samples pose a problem in accurate assessing of AG [23]. The low agreement between pathologists in diagnosing atrophy leads to the development of a staging system based on the evaluation of IM [operative link on gastric intestinal metaplasia (OLGIM) assessment] [24–26]. According to current evidence, the high agreement in the diagnosis of IM warrants their utilization as a more reliable marker for the prediction of gastric cancer risk in patients with premalignant gastric lesions [27]. The NBI-ME assessment of IM appears to be more accurate than AG in our study, which uses histological confirmation as the gold standard.

Regarding the analysis of areas displaying irregular pit pattern mucosa and/or vascular patterns, both of these endoscopic features showed a good correlation with dysplasia. We obtained a good diagnostic accuracy (91.1%), sensitivity and specificity (AUROC 0.87) of type C pattern for dysplasia. Mucosal and vascular disturbances are common endoscopic criteria both for dysplasia and for gastric cancer. The disappearance of fine mucosal structure, the irregular surface pattern and irregular vessels, are distinct endoscopic features associated with neoplastic lesions [28–30].

Our research proved the strength of NBI-ME in the real-time evaluation of intestinal metaplasia and dysplasia. Optical diagnosis may help the endoscopist to establish the topography and extent of premalignant gastric lesions and to select high-risk patients for further surveillance. This can minimize biopsies and reduce the burden for histology departments. Targeted biopsies should be performed only from those suspicious lesions with irregular, distorted patterns, which correspond with neoplastic transformation.

According to European guidelines, endoscopic surveillance should be offered to patients with extensive, severe IM and/or AG, and to patients with dysplasia [30]. We identified 16 patients with extensive IM and/or extensive AG (13 patients), and six patients with dysplasia by performing a targeted endoscopic and histological assessment.

When we compare our data with previous published reports, we conclude that training and expertise in identifying specific NBI endoscopic patterns are mandatory to improve diagnostic skills. The results achieved by the experts can be replicated in clinical practice with sufficient training programs [31]. A protocol based on optical biopsy meaning a thorough examination of the mucosa with less biopsies, may replace in the future the standard approach for the detection of premalignant gastric lesions.

Conclusions

The optical biopsy method is useful in the detection and characterization of gastric lesions. Our data suggest that using NBI-ME would facilitate the identification of patients at high-risk for developing gastric cancer, with a diminished histopathologist workload. Progress in this field is encouraging, but the benefit for patients is dependent upon clinical availability, the level of local expertise, and the standardization of endoscopic criteria.

Conflict of interests

The authors declare that they have no conflict of interests.

Acknowledgments

This paper is partially supported by the Internal Research Grant CIGCS UMF TGM-PO-CC-01-F01, financed by the University of Medicine and Pharmacy of Tîrgu Mureş, Romania.

References

[1] Correa P. Human gastric carcinogenesis: a multistep and multifactorial process – First American Cancer Society Award Lecture on Cancer Epidemiology and Prevention. Cancer Res, 1992, 52(24):6735–6740.

[2] de Vries AC, van Grieken NC, Looman CW, Casparie MK, de Vries E, Meijer GA, Kuipers EJ. Gastric cancer risk in patients with premalignant gastric lesions: a nationwide cohort study in the Netherlands. Gastroenterology, 2008, 134(4): 945–952.

[3] Pang SH, Leung WK, Graham DY. Ulcers and gastritis. Endoscopy, 2008, 40(2):136–139.

[4] de Vries AC, Haringsma J, de Vries RA, Ter Borg F, van Grieken NC, Meijer GA, van Dekken H, Kuipers EJ. Biopsy strategies for endoscopic surveillance of pre-malignant gastric lesions. *Helicobacter*, 2010, 15(4):259–264.

[5] Gheorghe C. Narrow-band imaging endoscopy for diagnosis of malignant and premalignant gastrointestinal lesions. J Gastrointestin Liver Dis, 2006, 15(1):77–82.
[6] Rey JF, Kuznetsov K, Lambert R. Narrow band imaging: a wide field of possibilities. Saudi J Gastroenterol, 2007, 13(1):1–10.
[7] Lambert R, Kuznetsov K, Rey JF. Narrow-band imaging in digestive endoscopy. ScientificWorldJournal, 2007, 7:449–465.
[8] Capelle LG, Haringsma J, de Vries AC, Steyerberg EW, Biermann K, van Dekken H, Kuipers EJ. Narrow band imaging for the detection of gastric intestinal metaplasia and dysplasia during surveillance endoscopy. Dig Dis Sci, 2010, 55(12): 3442–3448.
[9] Kim HH, Park MI, Choi JM, Park SJ, Moon W. Efficacy of narrow band imaging system combined with magnifying endoscopy for differentiating type IIa early gastric cancer from adenoma. Gastroenterology Res, 2011, 4(5):210–215.
[10] Ezoe Y, Muto M, Uedo N, Doyama H, Yao K, Oda I, Kaneko K, Kawahara Y, Yokoi C, Sugiura Y, Ishikawa H, Takeuchi Y, Kaneko Y, Saito Y. Magnifying narrowband imaging is more accurate than conventional white-light imaging in diagnosis of gastric mucosal cancer. Gastroenterology, 2011, 141(6): 2017–2025.e3.
[11] Rerknimitr R, Imraporn B, Klaikeaw N, Ridtitid W, Jutaghokiat S, Ponauthai Y, Kongkam P, Kullavanijaya P. Non-sequential narrow band imaging for targeted biopsy and monitoring of gastric intestinal metaplasia. World J Gastroenterol, 2011, 17(10):1336–1342.
[12] Dixon MF, Genta RM, Yardley JH, Correa P. Classification and grading of gastritis. The updated Sydney System. International Workshop on the Histopathology of Gastritis, Houston, 1994. Am J Surg Pathol, 1996, 20(10):1161–1181.
[13] Lauwers GY, Carneiro F, Graham DY. Gastric carcinoma. In: Bosman FT, Carneiro F, Hruban RH, Theise ND (ed). World Health Organization (WHO) Classification of tumours of the digestive system. 4th edition, International Agency for Research on Cancer (IARC) Press, Lyon, 2010, 48–58.
[14] Maki S, Yao K, Nagahama T, Beppu T, Hisabe T, Takaki Y, Hirai F, Matsui T, Tanabe H, Iwashita A. Magnifying endoscopy with narrow-band imaging is useful in the differential diagnosis between low-grade adenoma and early cancer of superficial elevated gastric lesions. Gastric Cancer, 2013, 16(2):140–146.
[15] Pimentel-Nunes P, Dinis-Ribeiro M, Soares JB, Marcos-Pinto R, Santos C, Rolanda C, Bastos RP, Areia M, Afonso L, Bergman J, Sharma P, Gotoda T, Henrique R, Moreira-Dias L. A multicenter validation of an endoscopic classification with narrow band imaging for gastric precancerous and cancerous lesions. Endoscopy, 2012, 44(3):236–246.
[16] Pimentel-Nunes P, Libânio D, Lage J, Abrantes D, Coimbra M, Esposito G, Hormozdi D, Pepper M, Drasovean S, White JR, Dobru D, Buxbaum J, Ragunath K, Annibale B, Dinis-Ribeiro M. A multicenter prospective study of the real-time use of narrow-band imaging in the diagnosis of premalignant gastric conditions and lesions. Endoscopy, 2016, 48(8):723–730.
[17] Uedo N, Ishihara R, Iishi H, Yamamoto S, Yamamoto S, Yamada T, Imanaka K, Takeuchi Y, Higashino K, Ishiguro S, Tatsuta M. A new method of diagnosing gastric intestinal metaplasia: narrow-band imaging with magnifying endoscopy. Endoscopy, 2006, 38(8):819–824.
[18] Song J, Zhang J, Wang J, Guo X, Wang J, Liu Y, Dong W. Meta-analysis: narrow band imaging for diagnosis of gastric intestinal metaplasia. PLoS One, 2014, 9(4):e94869.
[19] Tahara T, Shibata T, Nakamura M, Yoshioka D, Arisawa T, Hirata I. Light blue crest sign, a favorable marker for predicting the severity of gastric atrophy in the entire stomach. Endoscopy, 2008, 40(10):880.
[20] Anagnostopoulos GK, Ragunath K, Shonde A, Hawkey CJ, Kenshi Y. Diagnosis of autoimmune gastritis by high resolution magnification endoscopy. World J Gastroenterol, 2006, 12(28): 4586–4587.
[21] Kawamura M, Abe S, Oikawa K, Terai S, Saito M, Shibuya D, Kato K, Shimada T, Uedo N, Masuda T. Topographic differences in gastric micromucosal patterns observed by magnifying endoscopy with narrow band imaging. J Gastroenterol Hepatol, 2011, 26(3):477–483.
[22] Haber MM. Gastric biopsies: increasing the yield. Clin Gastroenterol Hepatol, 2007, 5(2):160–165.
[23] el-Zimaity HM, Graham DY, al-Assi MT, Malaty H, Karttunen TJ, Graham DP, Huberman RM, Genta RM. Interobserver variation in the histopathological assessment of *Helicobacter pylori* gastritis. Hum Pathol, 1996, 27(1):35–41.
[24] Chen XY, van der Hulst RW, Bruno MJ, van der Ende A, Xiao SD, Tygat GN, Ten Kate FJ. Interobserver variation in the histopathological scoring of *Helicobacter pylori* related gastritis. J Clin Pathol, 1999, 52(8):612–615.
[25] Offerhaus GJ, Price AB, Haot J, ten Kate FJ, Sipponen P, Fiocca R, Stolte M, Dixon MF. Observer agreement on the grading of gastric atrophy. Histopathology, 1999, 34(4):320–325.
[26] Capelle LG, de Vries AC, Haringsma J, Ter Borg F, de Vries RA, Bruno MJ, van Dekken H, Meijer J, van Grieken NC, Kuipers EJ. The staging of gastritis with the OLGA system by using intestinal metaplasia as an accurate alternative for atrophic gastritis. Gastrointest Endosc, 2010, 71(7):1150–1158.
[27] Yao K, Anagnostopoulos GK, Ragunath K. Magnifying endoscopy for diagnosing and delineating early gastric cancer. Endoscopy, 2009, 41(5):462–467.
[28] Kaise M, Kato M, Urashima M, Arai Y, Kaneyama H, Kanzazawa Y, Yonezawa J, Yoshida Y, Yoshimura N, Yamasaki T, Goda K, Imazu H, Arakawa H, Mochizuki K, Tajiri H. Magnifying endoscopy combined with narrow-band imaging for differential diagnosis of superficial depressed gastric lesions. Endoscopy, 2009, 41(4):310–315.
[29] Li HY, Dai J, Xue HB, Zhao YJ, Chen XY, Gao YJ, Song Y, Ge ZZ, Li XB. Application of magnifying endoscopy with narrow-band imaging in diagnosing gastric lesions: a prospective study. Gastrointest Endosc, 2012, 76(6):1124–1132.
[30] Dinis-Ribeiro M, Areia M, de Vries AC, Marcos-Pinto R, Monteiro-Soares M, O'Connor A, Pereira C, Pimentel-Nunes P, Correia R, Ensari A, Dumonceau JM, Machado JC, Macedo G, Malfertheiner P, Matysiak-Budnik T, Megraud F, Miki K, O'Morain C, Peek RM, Ponchon T, Ristimaki A, Rembacken B, Carneiro F, Kuipers EJ; European Society of Gastrointestinal Endoscopy; European *Helicobacter* Study Group; European Society of Pathology; Sociedade Portuguesa de Endoscopia Digestiva. Management of precancerous conditions and lesions in the stomach (MAPS): guideline from the European Society of Gastrointestinal Endoscopy (ESGE), European *Helicobacter* Study Group (EHSG), European Society of Pathology (ESP), and the Sociedade Portuguesa de Endoscopia Digestiva (SPED). Endoscopy, 2012, 44(1):74–94.
[31] Dias-Silva D, Pimentel-Nunes P, Magalhães J, Veloso N, Ferreira C, Figueiredo P, Moutiho P, Dinis-Ribeiro M. The learning curve for narrow-band imaging in the diagnosis of precancerous gastric lesions by using Web-based video. Gastrointest Endosc, 2014, 79(6):910–920.

Corresponding author
Alina Mioara Boeriu, Associate Professor, MD, PhD, Department of Gastroenterology, University of Medicine and Pharmacy of Tîrgu Mureş, 38 Gheorghe Marinescu Street, 540139 Tîrgu Mureş, Mureş County, Romania; Phone +40722–298 111, e-mail: aboeriu@gmail.com

Received: October 18, 2017 *Accepted: August 9, 2018*